# Integrated modelling of reactions between energetic particles and metal wall impurities in tokamak plasmas

Ž. Štancar[1], J. Eriksson[1], H.J.C. Oliver[1], V.G. Kiptily[1], S. Conroy[2], A. Čufar[3], A. Hjalmarsson[2], Ye.O. Kazakov[4], Z. Ghani[1], M. Gorelenkova[5], A. Boboc[1], P. Carvalho[1], A. Chomiczewska[6], E. Delabie[7], M. Dreval[8], L. Garzotti[1], K.K. Kirov[1], D. Kos[1], K. D. Lawson[1], I. Lengar[3], M. Lennholm[1], E. Lerche[4], X. Litaudon[9], E. Litherland-Smith[1], M. Maslov[1], S. Menmuir[1], M. O'Mullane[1], E. Parr[1], A. Patel[1], L. Snoj[3], R. Sydenham[10], H.J. Sun[1], R. Villari[11], V.T. Wang[12], V.K. Zotta[13], and JET Contributors*

[1] *United Kingdom Atomic Energy Authority, Culham Campus, UK*
[2] *Department of Physics and Astronomy, Uppsala University, Sweden*
[3] *Jožef Stefan Institute, Ljubljana, Slovenia*
[4] *Laboratory for Plasma Physics, Ecole Royale Militaire, Brussels, Belgium*
[5] *Princeton Plasma Physics Laboratory, Princeton, USA*
[6] *Institute of Plasma Physics and Laser Microfusion, Warsaw, Poland*
[7] *Oak Ridge National Laboratory, Oak Ridge, USA*
[8] *National Science Centre, Kharkiv Institute of Physics and Technology, Kharkiv, Ukraine*
[9] *CEA, Cadarache, France*
[10] *University of Portsmouth, Portsmouth, UK*
[11] *C.R. ENEA Frascati, Frascati, Italy*
[12] *Queen Mary University, London, UK*
[13] *Dipartimento di Ingegneria Astronautica, Elettrica ed Energetica, University of Rome La Sapienza Faculty of Engineering, Rome, Italy*
* *See the author list of 'Overview of T and D-T results in JET with ITER-like wall' by CF Maggi et al 2024 Nucl. Fusion 64 112012*

## Introduction

Fusion power measurements are an essential tokamak operational parameter, relevant for radiation safety, fuel self-sufficiency, plasma diagnostics, and for validating progress towards high-gain scenarios. Yields are absolutely calibrated via elaborate in-vessel procedures supported by neutronics calculations, the accuracy of which depends on the fidelity of the underlying plasma neutron source and transport models; analogous in-situ calibrations are foreseen for SPARC, ITER, and DEMO. Over the past decade, coupled plasma–neutronics integrated modelling workflows have been developed and validated for tokamaks, combining plasma transport solvers, fusion kinematics codes, and Monte Carlo neutron and photon transport codes [1, 2, 3]. They generate high-fidelity, radially and poloidally resolved emissivity profiles with pitch-dependent energy spectra, used for diagnostic optimization, shielding and radiation-safety studies, and surrogate fusion-performance models.

Here we extend these workflows to the non-standard proton–beryllium (*p–Be*) fusion chain, validated with dedicated experiments triggering reactions between fast ions and the beryllium impurities intrinsic to JET's ITER-like wall (ILW, metal Be/W). The relevant reactions are:

I.a) $^{9}$Be(p,n)$^{9}$B ($Q=-1.85$); I.b) $^{9}$Be(p,$\alpha$)$^{6}$Li ($Q=2.13$); I.c) $^{9}$Be(p,d)2$\alpha$ ($Q=0.65$)
II.a) $^{9}$Be(d,n)$^{10}$B ($Q=4.36$); II.b) $^{9}$Be($\alpha$,n)$^{12}$C ($Q=5.70$) [MeV]

Of the primary reactions only the endothermic $^{9}$Be(p,n)$^{9}$B (threshold $\approx 2.06$ MeV) emits neutrons, so neutron production requires suprathermal, MeV-range protons. The charged products of $^{9}$Be(p,$\alpha$)$^{6}$Li and $^{9}$Be(p,d)2$\alpha$ are confined, slow down, and drive secondary neutron-emitting fusion on beryllium [II.a, II.b]. Neutron emission is thus a two-stage process whose primary/secondary balance depends strongly on the fast-proton energy distribution. The work is driven by three goals: *(i)* design a steady-state scenario for studying fusion products from reactions between fast ions and metallic wall impurities, exploiting the Be naturally present in JET's

ILW [4]; *(ii)* demonstrate and experimentally validate the modelling of non-standard fusion products [5], providing high-fidelity source terms to energetic-particle, synthetic-diagnostic, and neutron-transport codes; and *(iii)* re-evaluate and validate cross sections for fusion between fast ions and beryllium.

**Experimental observations**

Dedicated experiments were performed in JET's 2022 *C43* He and 2023 *C45* D campaigns. An energetic proton population was generated by fundamental-frequency RF heating of a puffed H minority ($P_{RF} = 4$–$5$ MW, $I_p = 1.45$ MA, $B_0 = 2.2$–$2.8$ T), while Be was intrinsically present from the metal wall. Plasma density was minimized to grow the fast-proton tail and raise the (H+Be)/$n_e$ ratio, and no NBI was applied (except diagnostic blips in D) to keep the plasmas in L-mode and avoid parasitic absorption. He discharges reached steady-state neutron rates of $R_n \approx 6 \cdot 10^{13}$ s$^{-1}$ sustained over $\geq 5$ s – the highest of the *C43* campaign, exceeding its average by more than three orders of magnitude (Fig. 1). The scenario was optimised by maximising RF power per proton and minimising collisionality through the density, magnetic-field, and RF-power actuators.

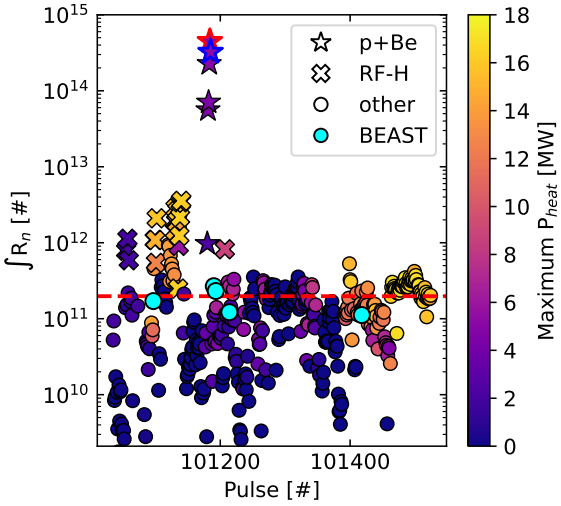


Figure 1: Time-integrated neutron yield across JET's 2022 *C43* He campaign; targeted *p–Be* pulses (stars) exceed the campaign mean (red dashed) by >3 orders of magnitude.

*p–Be* dominance in the selected discharges was established against two criteria. *(i) MeV-range fast protons present, fast deuterons and alphas absent:* the neutral particle analyser (NPA) measured a proton tail extending beyond 1 MeV with the combined D/$\alpha$ channel $\sim$3 orders of magnitude lower; the fast ion loss detector (FILD) recorded prompt proton losses from 0.7 to $>$ 3.5 MeV with no fusion-product loss signature; and magnetic coils showed Alfvén eigenmodes (TAEs, EAEs, NAEs) and fishbones driven by the energetic protons. *(ii) Fusion-product signatures:* provided by the $LaBr_3$ gamma spectrometers and the absolutely calibrated fission chambers.

A unique measurement came from JET's $LaBr_3$ gamma spectrometers (Fig. 2). The He and D spectra show a landmark peak at 3.56 MeV from $^9$Be(p,$\alpha\gamma$)$^6$Li – whose cross section closely mirrors that of $^9$Be(p,n)$^9$B, making it a proxy for the primary neutron emitter – providing direct evidence of a MeV-range proton population. The alpha-induced $^9$Be($\alpha$,n$\gamma$)$^{12}$C peak at 4.44 MeV lies almost two orders of magnitude lower, confirming that the fusion-alpha density, and hence secondary $\alpha$–Be fusion, was very small. The time-integrated gamma yield tracks the calibrated neutron rate within uncertainty, confirming that the same primary *p–Be* fusion drives both signals.

## Integrated modelling

A five-step integrated modelling framework was developed for the two-stage *p–Be* chain (Fig. 3). Interpretive TRANSP (TORIC–FPP) computes the RF H-minority distribution, while predictive JETTO-SANCO impurity-transport modelling fixes the plasma composition by matching the (extraordinarily high) $Z_{\mathrm{eff}} \approx 5$ (He) / 4 (D) and $P_{\mathrm{rad}}$. The proton distribution function is passed to LOCUST-GPU for full-orbit tracking, correcting for prompt losses and finite Larmor radius; DRESS then resolves the primary *p–Be* fusion kinematics. Birth deuterons and alphas are slowed down in LOCUST and looped back through DRESS for the secondary $^{9}$Be(d,n)$^{10}$B and $^{9}$Be($\alpha$,n)$^{12}$C reactions, before the combined source is transported in MCNP.

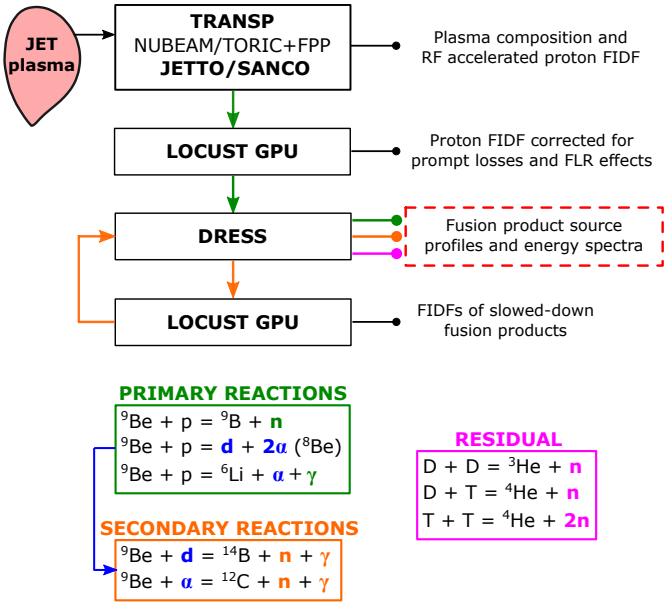


Figure 3: Five-step workflow modelling the two-stage *p–Be* chain: primary (green) and secondary (orange) fusion stages, plus the residual D/T contribution (violet).

LOCUST removes the counter-passing protons above $\approx 4$ MeV and predicts that $\approx 25\%$ of the simulated protons are promptly lost to the outboard Be limiters at the FILD location; the resulting FILD-like loss distribution reproduces the measured pitch-angle and energy structure, validating the fast-ion model. The residual discrepancy is attributed to MHD-enhanced losses, which are not captured by the modelling.

The primary $^{9}$Be(p,n)$^{9}$B reaction is confirmed as the dominant neutron emitter at the naturally present Be concentrations, with the secondary reactions $\approx 4$ orders of magnitude lower; the emissivity forms a hollow ring $\approx 15$ cm around the magnetic axis. In D discharge #105453, *p–d* knock-on acceleration combined with second-harmonic RF heating generates a fast-deuteron

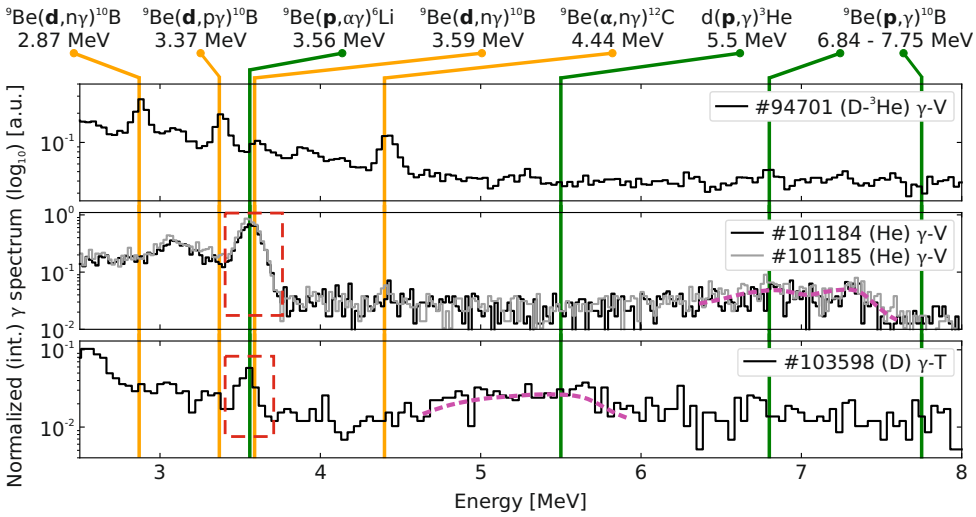


Figure 2: Normalized gamma spectra ($\gamma$-V vertical, $\gamma$-T tangential $LaBr_3$) for the D-$^{3}$He three-ion pulse #94701, He pulses #101184 and #101185, and D pulse #103598. Coloured lines mark gamma peaks from fast protons (green) and from deuterons/alphas (orange); red dashed rectangles highlight the primary *p–Be* peaks.

tail whose D–D and D–T fusion contributes $\approx 25\%$ of the total neutron rate, captured with a semi-empirical NPA-constrained model.

Calculated total neutron rates agree with the absolutely calibrated fission chambers within the combined experimental and computational uncertainty for all discharges, with an average discrepancy of $\approx \pm 20\%$ (Fig. 4) – comparable to the $\approx 40\%$ typical of fast–thermal-ion-driven D–D and D–T plasmas [3] – validating both the framework and the newly evaluated Be cross sections. Propagating the source through JET's MCNP model shows that the $^{235}$U fission-chamber response to *p–Be* neutrons is up to $\approx 10\%$ lower than to a generic D–D source, owing to the response-function dip between the D–D peak and $\approx 6$ MeV where the *p–Be* spectrum is most prominent. Multi-foil neutron activation ($^{115}$In, $^{27}$Al, $^{56}$Fe) is shown to resolve the spectral-tail energy gradients set by the fast-proton distribution.

## Conclusions

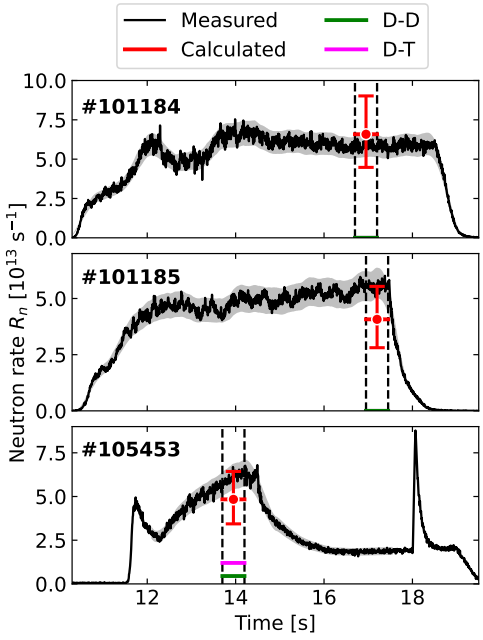


Figure 4: Measured versus calculated total neutron rates $R_n$ for #101184, #101185, and #105453 (D–D/D–T contribution added). Grey band: experimental uncertainty; red bars: computational uncertainty.

For the first time, a steady-state L-mode plasma with dominant proton–beryllium fusion and neutron yields up to $\approx 6 \cdot 10^{13}$ s$^{-1}$ has been demonstrated – sustained over several fast-ion slowing-down times – in both "aneutronic" He and bulk D, confirming the predictions made for ITER's Pre-Fusion Power Operation phase [5]. Exploiting the intrinsic metal-wall impurities, such scenarios can be used for early nuclear-diagnostic commissioning and energetic-particle confinement studies. The integrated modelling framework reproduces the measured neutron yield within $\approx \pm 20\%$ and matches the FILD loss distributions, demonstrating an ability to accurately model non-standard fusion reactions and to produce high-fidelity fusion-product source terms.

Following ITER's move to a full-tungsten wall with boronization, we applied the framework to fast-proton–boron interactions. In JET conditions the $^{11}$B(p,$\alpha$)2$\alpha$ alpha rate is $\approx 2\times$ that of *p–Be*, with a three-alpha rate comparable to D-$^3$He fusion. $^{11}$B(p,$\alpha$)2$\alpha$ could therefore provide a steady-state source of DT-like alphas for early $\alpha$-confinement studies, well ahead of D–T operation, while its low secondary neutron and gamma emission keeps the radiation-safety burden small – making it compatible with aneutronic commissioning discharges aimed at nuclear-diagnostic calibration and fusion-product studies.


## Acknowledgements

This work has been carried out within the framework of the EUROfusion Consortium, funded by the European Union via the Euratom Research and Training Programme (Grant Agreement No 101052200 — EUROfusion) and from the EPSRC [grant number EP/W006839/1]. Views and opinions expressed are however those of the author(s) only and do not necessarily reflect those of the European Union or the European Commission. Neither the European Union nor the European Commission can be held responsible for them.


## References


[1] Ž. Štancar *et al*, Nucl. Fusion **59**, 9 (2019)
[2] Ž. Štancar *et al*, Nucl. Fusion **61**, 12 (2021)
[3] Ž. Štancar *et al*, Nucl. Fusion **63**, 12 (2023)
[4] A. Krasilnikov *et al*, Nucl. Fusion **58**, 2 (2018)
[5] A. Polevoi *et al*, Nucl. Fusion **61**, 7 (2021)